PAPER

Highly effective capture and subsequent catalytic transformation of low-concentration CO_2 by superbasic guanidines†

Hui Zhou, [ID] * Wei Chen, Ji-Hong Liu, Wen-Zhen Zhang [ID] and Xiao-Bing Lu [ID] *

Herein, we present a highly efficient and convenient approach for carbon dioxide (CO_2) capture and catalytic transformation under mild conditions using N,N'-bis(imidazolyl)guanidines (BIGs, organoguanidine-based strong superbases) as the organocatalyst, even from simulated flue gas (10% CO_2/90% N_2, v/v) or directly from dry air (~400 ppm CO_2). The zwitterionic BIG–CO_2 adducts were successfully isolated and characterized. X-ray single crystal analysis revealed the bent geometry of the binding CO_2 in the BIG–CO_2 adduct with an O–C–O angle of 129.7° and increased C–O bond distances (1.253 and 1.237 Å) in comparison with free CO_2. Notably, the resulting BIG–CO_2 adducts were found to be capable of catalyzing the novel cycloaddition of various propiolamidines with simulated flue gas to generate functionalized ($4E,5Z$)-4-imino-5-benzylideneoxazolidine-2-ones in good yields and excellent selectivity.

Introduction

Nitrogen base-involving carbon dioxide (CO_2) capture and sequestration (CCS), as a kind of climate change mitigation technology, has attracted so much global attention with the aim of reducing anthropogenic CO_2 emissions.[1] Understanding the interaction pattern of nitrogen bases and CO_2 is critical to boost the development of CCS technology (Scheme 1). As is well known, primary and secondary amines could react with CO_2 by rapid nucleophilic attack to form zwitterionic nitrogen base–CO_2 adducts (N–CO_2 adducts). Due to the inherent instability, N–CO_2 adducts easily react with another molecule of an amine *via* a proton transfer process to form stable ammonium carbamate salts (Scheme 1, I). This method has been widely applied to remove CO_2 from highly concentrated and stationary CO_2 emission sources, such as power plants and industrial sectors.[2] In 2010, the first N–CO_2 adduct derived from 1,5,7-triazabicyclo[4.4.0]dec-5-ene (TBD) was successfully isolated and characterized by the Villiers group.[3] Note that X-ray single-crystal diffraction data indicate that the intramolecular hydrogen bonding leads to an increased stability of TBD–CO_2 adducts (Scheme 1, II). With the assistance of

Lewis acids, N–CO_2 adducts could also be stabilized, thus generating cyclic frustrated Lewis pair (FLP)–CO_2 adducts (Scheme 1, III).[4] Furthermore, N-heterocyclic imines (NHI) as more electron-rich nitrogen donors were recently developed to activate the pressured CO_2 by the Dielmann group and the corresponding stable NHI–CO_2 adducts were obtained through a nucleophilic attack process (Scheme 1, IV).[5]
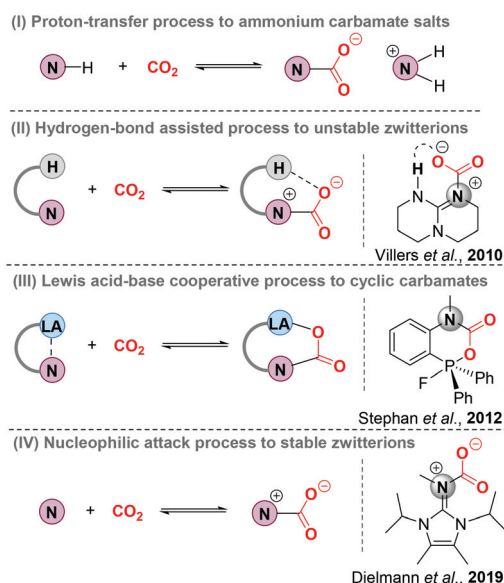
Scheme 1 Representative methods for CO_2 capture and sequestration by nitrogen base derivatives.

State Key Laboratory of Fine Chemicals, Dalian University of Technology, Dalian 116024, China. E-mail: zhouhui@dlut.edu.cn, xblu@dlut.edu.cn

Obviously, the donor strength of Lewis bases is a vital factor for CO_2 activation and sequestration. As a consequence, a series of Lewis base–CO_2 adducts have been synthesized,[6] employing strong basic carbon,[7] phosphine,[8] and oxygen bases.[9] N,N′-Bis(imidazolyl)guanidine (BIG) bases, formed by direct attachment of imidazolyl substituents to guanidine derivatives, have emerged as a new class of nitrogen bases.[10] Importantly, the pK_a values of the resulting BIG bases were determined to be between 26.1 and 29.3 in THF. Although commonly known organoguanidines have widely been applied for CO_2 capture, activation, and chemical transformation,[11] no literature regarding the use of strong basic BIG systems for CO_2 capture and sequestration has been reported. Herein, we report the synthesis, isolation and structural characterization of zwitterionic BIG–CO_2 adducts via a nucleophilic addition process. More importantly, this system is even effective in extracting CO_2 from the ambient air. Additionally, we demonstrate that BIG–CO_2 adducts also have the ability to catalyze the novel cycloaddition of propiolamidines with simulated flue gas to selectively form functionalized (4E,5Z)-4-imino-4-imino-5-benzylideneoxazolidine-2-ones with high activity.

Results and discussion

Synthesis and characterization of BIG–CO_2 adducts

Firstly, BIG hydrotetrafluoroborates **1a–1d** were synthesized as previously reported by Ullrich Jahn et al.[10a] BIG bases were prepared by the deprotonation of **1a–1d** with $KN(SiMe_3)_2$ in THF solution and further purified by extraction with n-hexane. When the n-hexane solution of BIG bases **2a–2d** was placed under an atmosphere of pure CO_2 at room temperature, white precipitates of BIG–CO_2 adducts (**3a–3d**) were rapidly formed and isolated in good to excellent yields (Scheme 2).

Furthermore, BIG–CO_2 adducts (**3a–3d**) were structurally characterized by ^{1}H NMR, ^{13}C NMR, IR and MS (ESI).† ^{13}C NMR spectra of **3a–3d** show the chemical shifts of the carbonyl group in the range of 162.1–162.3 ppm, which are quite close
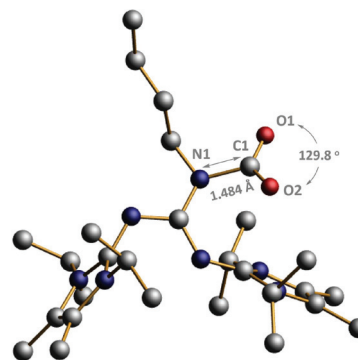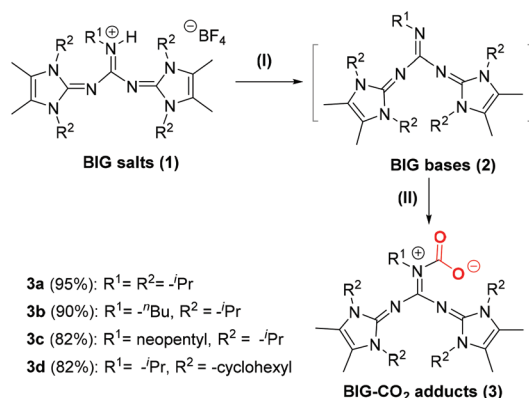

Fig. 1 POV-Ray illustrations of the molecular structure of BIG–CO_2 adduct **3b**. Hydrogen atoms have been omitted for clarity. C: black, O: red, and N: dark blue. Selected bond lengths (Å) and angles (°): N1–C1, 1.484(6); O1–C1, 1.253(6); O2–C1, 1.237(4); O1–C1–O2, 129.78(7).

to those of reported NHI–CO_2 adducts.[10a] Meanwhile, a ^{13}C isotope labeling experiment was conducted, in which the CO_2 resonance of **3a** (162.1 ppm) obtained from [13]CO_2 was enhanced obviously. And also, the C=O stretching frequencies of **3a–3d** were investigated in the range of 1610–1631 cm^{-1}. Gratifyingly, the single crystal of **3a** was obtained and determined by X-ray single crystal diffraction, as shown in Fig. 1. The crystal structure data show that the C1–O1 and C1–O2 bond distances, 1.253(6) and 1.237(4) Å, respectively, are both elongated, in comparison with that of free gaseous CO_2 (1.160 Å). A bent geometry of the binding CO_2 with an O1–C1–O2 angle of 129.78(7)° was observed in the BIG–CO_2 adduct, indicating that CO_2 is activated through nucleophilic attack by BIG bases. Moreover, the dihedral angles between the plane of the guanidine core and the two imidazole planes are 109.85 (4)° and 119.54(4)°, respectively.

In addition, the thermal stability of BIG–CO_2 adducts **3a–3d** was investigated by means of thermogravimetric analysis (TGA). From the results (ESI, Fig. S1–S4†), the reversible decarboxylation of **3a–3d** began in the range of 129.2–135.8 °C, and the observed weight losses were matched well with the theoretical content of CO_2 in BIG–CO_2 adducts.

CO_2 capture ability of BIG bases under various concentrations of CO_2

Reversible CO_2 capture and release of BIG bases was also studied by Density Functional Theory (DFT) calculations (ESI, Fig. S5†). The free energy barriers of BIG bases **2a–2d** for CO_2 capture are very low (5.5–7.6 kcal mol^{-1}), and the formation of BIG–CO_2 adducts **3a–3c** is even more exergonic. Based on this observation, BIG bases have the potential to be applied for CO_2 activation and capture. Up to now, most of the existing CCS technologies are applied in highly concentrated and stationary CO_2 emission sources. Direct CO_2 capture from ambient air, by contrast, is becoming more promising to permanently lower the atmospheric CO_2 concentration, thus achieving negative carbon emissions.[12] As shown in Fig. 2, the CO_2 capture ability of BIG bases with **2a** as an example was

3a (95%): R^1 = R^2 = -^{i}Pr
3b (90%): R^1 = -^{n}Bu, R^2 = -^{i}Pr
3c (82%): R^1 = neopentyl, R^2 = -^{i}Pr
3d (82%): R^1 = -^{i}Pr, R^2 = -cyclohexyl

Scheme 2 CO_2 activation and fixation by BIG bases. Reaction conditions: (I) $KN(SiMe_3)_2$, THF, 25 °C, 2 h; (II) CO_2 (1 atm), n-hexane, 25 °C, 2 h.
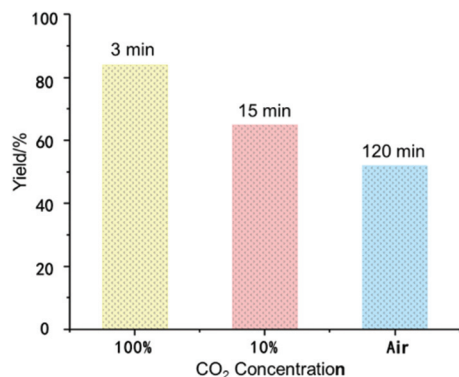
Fig. 2 CO_2 fixation ability of a BIG base (**2a**) under various concentrations of CO_2. Reaction conditions: BIG base (**2a**) (0.1 mmol), hexane (5 mL), 25 °C, CO_2 (balloon); simulated flue gas (100 mL min^{-1}); dry air (100 mL min^{-1}).

Scheme 3 COS/CS_2 activation and fixation by BIG bases.

Fig. 3 POV-Ray illustrations of the molecular structure of **6**. Hydrogen atoms have been omitted for clarity. C: black, S: yellow, and N: dark blue. Selected bond lengths (Å) and angles (°): N1–C1, 1.427(7); S1–C1, 1.703(6); S2–C1, 1.680(9); S1–C1–S2, 122.96(4).

measured under various concentrations of CO_2. When the commercially pure CO_2 was introduced with a balloon, a white precipitate was formed immediately to obtain **3a** in 84% isolated yield within 3 minutes. Moreover, CO_2 capture from simulated flue gas (10% CO_2/90% N_2, v/v) could also be carried out at a flow rate of 100 mL min^{-1}, and the corresponding **3a** was formed in 65% yield within 15 minutes. When switching to dry air containing about 400 ppm of CO_2, a yield of 52% could be obtained with an enhanced reaction time of 2 hours.

Protonation of BIG–CO_2 adducts in the presence of H_2O

Most of the known Lewis base–CO_2 adducts are sensitive to protic solvents, such as water and alcohols.[13] Surprisingly, recently reported NHI–CO_2 adducts bearing a methyl group at the exocyclic nitrogen atom showed unprecedented chemical stability towards hydrolysis, probably due to the hydrophobic nature of the CO_2 binding site.[5] The stability of BIG–CO_2 adducts toward water was also evaluated in THF solution at ambient temperature. In the presence of 1.2 equiv. H_2O, **2a–2c** was rapidly hydrolyzed via a decarboxylation process to form ammonium bicarbonates **4a–c** in 90–98% isolated yields. Meanwhile, the X-ray crystal structure of **4a** was also determined (ESI, Fig. S7†).

Application of BIG for COS and CS_2 capture and activation

Because of the structural similarity of COS and CS_2 molecules to CO_2,[14] their capture using BIG base **2a** was also investigated under the same reaction conditions. As shown in Scheme 3, the COS and CS_2 capture processes could smoothly proceed at room temperature and the corresponding BIG–COS adduct **5** and CS_2 adduct **6** were isolated in 97% and 98% yields, respectively. The solid-state structure of the BIG–CS_2 adduct **6** shows that CS_2 binds to the nitrogen atom with a N1–C1 bond of 1.427(7) Å and a S–C–S angle of 122.96(4)° (Fig. 3). Note that the BIG–CS_2 adduct **6** is the first example of a nitrogen-based zwitterionic adduct. The groups of Vlasse[15] and Jessop[16] independently reported the reaction of CS_2 with cyclic amidines to
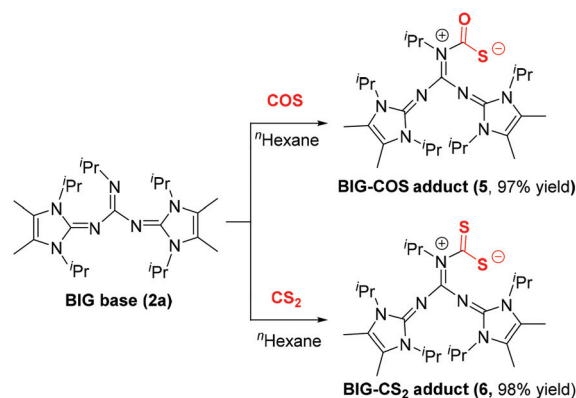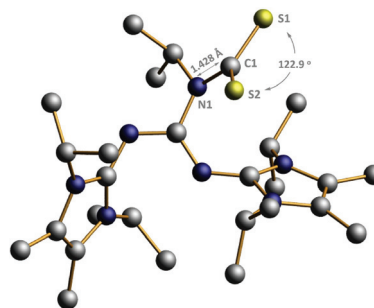
form cyclic carbamic carboxylic trithioanhydride rings, while acyclic acetamidines were cleaved by CS_2 at room temperature to give an isothiocyanate and a thioacetamide. In addition, Cantat et al. showed that TBD reacted with CS_2 and the guanidinium dithiocarbamate was selectively synthesized via a proton transfer process.[17]

Application of BIG–CO_2 adducts as organocatalysts for CO_2 catalytic transformation

As an additional CO_2-mitigation strategy to CCS, CO_2 capture and utilization (CCU) is attracting global interest.[18] Recently, Lewis base–CO_2 adducts,[6,19] as a new class of organic catalysts, have exhibited unique reactivity and selectivity for CO_2 transformation to value-added chemicals, which inspires us to further investigate the application of BIG–CO_2 adducts in the CCU process. Gratifyingly, BIG–CO_2 adduct **3b** could efficiently catalyze the novel cycloaddition of propargylamidine **7a** with simulated flue gas at 80 °C in 24 hours (for detailed optimized conditions, see ESI, Table S1†), thus generating 4-imino-5-benzylideneoxazolidine-2-one **8a** in 90% isolated yield. The reactions of propargylamidines (**7b–7f**) bearing methyl, methoxyl or halogen groups (–F, –Cl, and –Br) on the aryl ring gave the corresponding products **8b–8f** in moderate to excellent yields. When the R^2 group was transformed to the cyclohexyl group,

Table 1 BIG–CO₂ adduct **3b** catalyzed cycloaddition of propargylamidines with CO_2 (simulated flue gas)^a
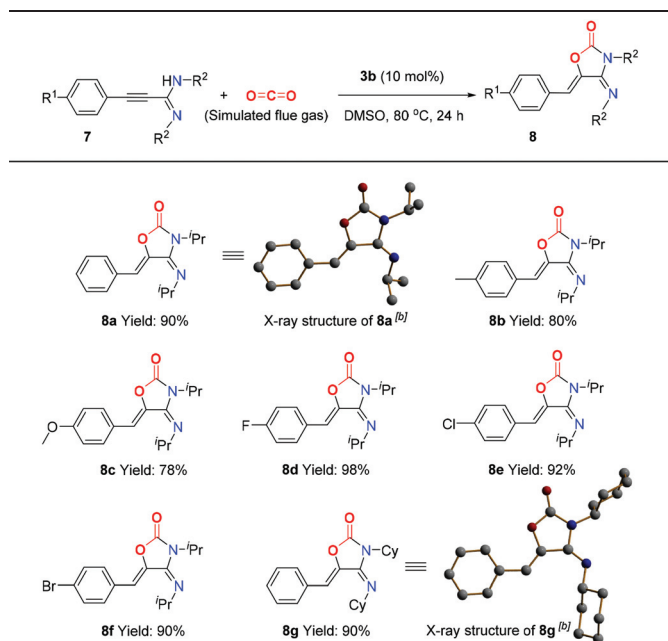
^{a} General reaction conditions: Sub. **7** (0.25 mmol), BIG–CO₂ adduct **3b** (0.025 mmol, 10 mol%), CO₂ balloon (10% CO₂, 90% N₂), DMSO (1.0 mL), 80 °C, 24 h. Isolated yields. ^{b} POV-ray depiction of single crystal. C: black, O: red, and N: dark blue.

the corresponding substrate **7g** was converted to **8g** with 90% yield. Meanwhile, the absolute stereostructures of (4*E*,5*Z*)-**8a** and **8g** were clearly confirmed by single-crystal X-ray diffraction study (Table 1).

To demonstrate the synthetic utility of this transformation, the gram-scale synthesis and further transformations of the products were next elucidated, as shown in Scheme 4. Under the standard conditions, the reaction of **7f** (1.2 g) with simulated flue gas proceeded smoothly, isolating the corresponding

Scheme 4 Gram-scale synthesis and synthetic applications of products.

product **8f** in 81% yield (Scheme 4, I). Moreover, the carbon–carbon double bond of product **8a** was selectively reduced by H_2 in the presence of Pd/C catalyst at room temperature, and the reduced product **9** was isolated in 95% yield (Scheme 4, **II**). Oxazolidine-2,4-diones, as a significant class of heterocyclic scaffolds, are frequently found in biologically active and medicinally useful molecules.[20] Note that the hydrolysis of **8f** could take place smoothly in an aqueous solution of hydrochloric acid, thus affording oxazolidine-2,4-dione **10** in 98% yield (Scheme 4, III).

Conclusions

In summary, we have demonstrated the high efficiency of superbasic guanidines for reversible capture of low-concentration CO₂ at room temperature and atmospheric pressure, affording the corresponding CO₂ adducts in good and excellent yields. Moreover, the resulting BIG–CO₂ adducts were demonstrated to be efficient organocatalysts for the cyclization of CO₂ (10% CO₂/90% N₂, v/v) and propiolamidines to produce various functionalized (4*E*,5*Z*)-4-imino-5-benzylideneoxazolidine-2-ones in high yields and excellent selectivity. The present study provides an alternative method for CO₂ capture and subsequent catalytic transformation of low-concentration CO₂ under mild conditions. Further explorations regarding the applications of organocatalytic systems for the synthesis of various heterocyclic chemicals are now in progress.

Experimental

Representative experimental procedure for the synthesis of BIG–CO₂ adducts (3a–3d)

In a nitrogen-filled glove box, BIG salt **1a** (545 mg, 1.0 mmol) was added to a suspension of KHMDS (199 mg, 1.0 mmol) in THF (10 mL) and the mixture was stirred at 25 °C for 2 h. Then the solvent was removed *in vacuo* and the residues were extracted with *n*-hexane (10 mL). After filtration to remove the inorganic salt, the filtrate was exposed to 1.0 atm of CO₂ at room temperature for 2 h. The resulting precipitates were collected *via* filtration, washed with *n*-hexane (3 × 5 mL) and then dried *in vacuo* to afford BIG–CO₂ adduct **3a** as a white solid (476 mg, 95% yield). **^{1}H NMR** (400 MHz, CDCl₃) δ 4.52 (dt, J = 14.1, 7.0 Hz, 4H), 4.06 (dt, J = 13.1, 6.5 Hz, 1H), 2.23 (s, 12H), 1.47 (d, J = 7.1 Hz, 24H), 1.21 (d, J = 6.5 Hz, 6H); **^{13}C NMR** (126 MHz, CDCl₃) δ 162.1, 156.2, 147.6, 120.2, 47.9, 44.0, 23.1, 21.3, 10.1. **IR** $\nu_{C=O}$: 1650 cm^{-1}. **HRMS (ESI)**: calcd for C₂₇H₄₇N₇O₂: 458.3966 [M − CO₂ + H]$^+$. Found: 458.3962 [M − CO₂ + H]$^+$.

3b. White solid (464 mg, 90% yield). **^{1}H NMR** (500 MHz, CDCl₃) δ 4.49 (dt, J = 14.1, 7.0 Hz, 4 H), 3.60–3.07 (m, 2H), 2.19 (s, 12H), 1.54 (dt, J = 15.0, 7.5 Hz, 2H), 1.44 (d, J = 7.0 Hz, 24H), 1.31 (dt, J = 15.0, 7.4 Hz, 2H), 0.86 (dt, J = 14.1, 7.2 Hz, 3H). **^{13}C NMR** (126 MHz, CDCl₃) δ 162.1, 157.4, 147.9, 120.1, 47.9, 42.3, 32.5, 21.3, 20.2, 13.9, 10.1. **IR** $\nu_{C=O}$: 1647 cm^{-1}.
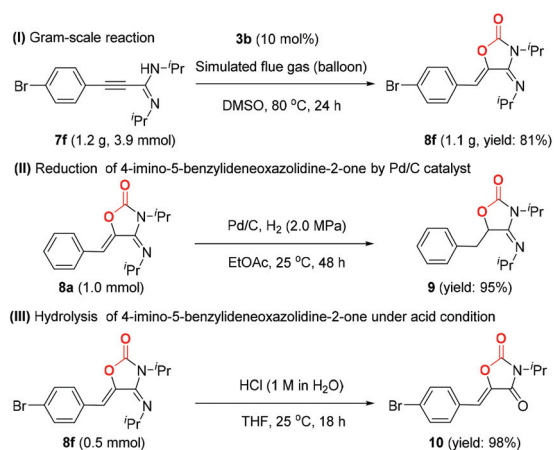
HRMS (ESI): calcd for $C_{28}H_{49}N_7O_2$: 472.4122 $[M - CO_2 + H]^+$. Found: 472.4155 $[M - CO_2 + H]^+$.

3c. White solid (434 mg, 82% yield). **¹H NMR** (400 MHz, CDCl₃) δ 4.76–4.24 (m, 4H), 3.23 (s, 2H), 2.25 (s, 12H), 1.48 (d, J = 7.1 Hz, 24H), 0.92 (s, 9H); **¹³C NMR** (101 MHz, CDCl₃) δ 162.2, 157.3, 147.6, 120.3, 53.6, 47.9, 32.2, 27.4, 21.4, 10.1. **IR** $\nu_{C=O}$: 1654 cm⁻¹. **HRMS (ESI):** calcd for $C_{29}H_{51}N_7O_2$: 486.4279 $[M - CO_2 + H]^+$. Found: 486.4271 $[M - CO_2 + H]^+$.

3d. White solid (542 mg, 82% yield). **¹H NMR** (400 MHz, CDCl₃) δ 4.19 (dt, J = 11.6, 5.6 Hz, 1H), 4.13–3.97 (m, 4H), 2.24 (s, 12H), 1.79 (dd, J = 62.7, 9.0 Hz, 28H), 1.44–0.99 (m, 18H); **¹³C NMR** (126 MHz, CDCl₃) δ 162.3, 155.3, 147.8, 120.6, 56.8, 44.1, 31.0, 26.2, 25.1, 23.5, 10.9. **IR** $\nu_{C=O}$: 1639 cm⁻¹. **HRMS (ESI):** calcd for $C_{39}H_{63}N_7O_2$: 618.5218 $[M - CO_2 + H]^+$. Found: 618.5205 $[M - CO_2 + H]^+$.

Representative experimental procedure for the cycloaddition of propiolamidines with simulated flue gas to (4E,5Z)-4-imino-5-benzylideneoxazolidine-2-ones

In a nitrogen-filled glove box, a 10 mL Schlenk flask equipped with a magnetic stirring bar was charged with propiolamidine **7a** (57.1 mg, 0.25 mmol), Cat. **3b** (12.9 mg, 0.025 mmol, 10 mol%) and DMSO (1.0 mL). Then the Schlenk flask was immediately transferred from the glovebox, and exchanged with CO₂ (10% CO₂/90% N₂, v/v) using a balloon. The reaction was stirred at 80 °C for 24 h. The crude reaction mixture was purified by column chromatography on silica gel (eluent: petroleum ether/ethyl acetate = 5 : 1) to give the desired (4E,5Z)-4-imino-5-benzylideneoxazolidine-2-one **8a** (61.2 mg, 90%) as a white solid. **¹H NMR** (400 MHz, CDCl₃) δ 7.77–7.63 (m, 2H), 7.39 (t, J = 7.4 Hz, 2H), 7.32 (t, J = 7.3 Hz, 1H), 6.35 (s, 1H), 4.10 (tt, J = 12.3, 3.9 Hz, 1H), 3.84 (t, J = 9.1 Hz, 1H), 2.21 (dq, J = 12.5, 3.3 Hz, 2H), 1.85 (d, J = 9.7 Hz, 6H), 1.68 (t, J = 11.8 Hz, 4H), 1.61–1.13 (m, 10H); **¹³C NMR** (101 MHz, CDCl₃) δ 152.7, 142.8, 136.1, 132.8, 130.5, 129.0, 128.9, 113.1, 57.0, 52.0, 33.9, 28.6, 26.1, 26.0, 25.3, 24.5. **IR**: 2930, 2855, 1797, 1670, 1647, 1450, 1367, 1331, 1232, 1201, 1089. **HRMS (ESI):** calcd for $C_{22}H_{28}N_2O_2$: 353.2224 $[M + H]^+$. Found: 353.2212 $[M + H]^+$.

8b. White solid (80%). **¹H NMR** (400 MHz, CDCl₃) δ 7.61 (d, J = 7.9 Hz, 2H), 7.20 (d, J = 7.9 Hz, 2H), 6.40 (s, 1H), 4.52 (hept, J = 6.8 Hz, 1H), 4.17 (hept, J = 6.1 Hz, 1H), 2.37 (s, 3H), 1.43 (d, J = 6.9 Hz, 6H), 1.28 (d, J = 6.1 Hz, 6H). **¹³C NMR** (101 MHz, CDCl₃) δ 152.5, 143.0, 139.4, 135.6, 130.5, 129.9, 129.6, 113.5, 49.0, 44.1, 24.1, 21.5, 19.0. **IR**: 2971, 2935, 1794, 1670, 1647, 1407, 1385, 1349, 1330, 1313, 1252, 1178, 1024. **HRMS (ESI):** calcd for $C_{17}H_{22}N_2O_2$: 287.1754 $[M + H]^+$. Found: 287.1752 $[M + H]^+$.

8c. White solid (78%). **¹H NMR** (400 MHz, CDCl₃) δ 7.67 (d, J = 8.9 Hz, 2H), 6.91 (d, J = 8.9 Hz, 2H), 6.38 (s, 1H), 4.69–4.36 (m, 1H), 4.32–4.08 (m, 1H), 3.84 (s, 3H), 1.42 (d, J = 6.9 Hz, 6H), 1.27 (d, J = 6.2 Hz, 6H). **¹³C NMR** (126 MHz, CDCl₃) δ 160.3, 152.6, 143.1, 134.8, 132.2, 125.5, 114.4, 113.3, 55.5, 49.0, 44.1, 24.1, 19.1. **IR**: 2957, 2927, 1793, 1670, 1646, 1604, 1513, 1408, 1385, 1256, 1178, 1026. **HRMS (ESI):** calcd for $C_{17}H_{22}N_2O_3$: 303.1703 $[M + H]^+$. Found: 303.1693 $[M + H]^+$.

8d. White solid (98%). **¹H NMR** (400 MHz, CDCl₃) δ 7.87–7.54 (m, 2H), 7.21–6.87 (m, 2H), 6.38 (s, 1H), 4.52 (hept, J = 7.0 Hz, 1H), 4.31–4.01 (m, 1H), 1.42 (d, J = 7.0 Hz, 6H), 1.27 (d, J = 6.2 Hz, 6H). **IR**: 2972, 1797, 1673, 1650, 1602, 1509, 1408, 1386, 1252, 1163, 1023. **HRMS (ESI):** calcd for $C_{16}H_{19}FN_2O_2$: 291.1503 $[M + H]^+$. Found: 291.1493 $[M + H]^+$.

8e. White solid (82%). **¹H NMR** (400 MHz, CDCl₃) δ 7.64 (d, J = 8.6 Hz, 2H), 7.35 (d, J = 8.6 Hz, 2H), 6.36 (s, 1H), 4.51 (m, J = 6.9 Hz, 1H), 4.30–4.00 (m, 1H), 1.42 (d, J = 7.0 Hz, 6H), 1.27 (d, J = 6.2 Hz, 6H). **¹³C NMR** (126 MHz, CDCl₃) δ 152.1, 142.6, 136.4, 134.9, 131.6, 131.3, 129.1, 111.9, 49.2, 44.3, 24.1, 19.0. **IR**: 2972, 1794, 1673, 1648, 1490, 1409, 1385, 1349, 1251, 1180, 1080, 1022. **HRMS (ESI):** calcd for $C_{16}H_{19}ClN_2O_2$: 307.1208 $[M + H]^+$. Found: 307.1198 $[M + H]^+$.

8f. White solid (90%). **¹H NMR** (400 MHz, CDCl₃) δ 7.50 (d, J = 8.5 Hz, 2H), 7.43 (d, J = 8.5 Hz, 2H), 6.27 (s, 1H), 4.44 (m, J = 6.9 Hz, 1H), 4.08 (m, J = 6.1 Hz, 1H), 1.35 (d, J = 6.9 Hz, 6H), 1.20 (d, J = 6.2 Hz, 6H). **¹³C NMR** (101 MHz, CDCl₃) δ 152.1, 142.6, 136.5, 132.1, 131.9, 131.7, 123.3, 112.0, 49.2, 44.2, 24.1, 19.0. **IR**: 2970, 2938, 1794, 1671, 1646, 1486, 1408, 1385, 1348, 1307, 1250, 1176, 1074, 1021. **HRMS (ESI):** calcd for $C_{16}H_{19}BrN_2O_2$: 351.0703 $[M + H]^+$. Found: 351.0693 $[M + H]^+$.

8g. White solid (90%). **¹H NMR** (400 MHz, CDCl₃) δ 7.77–7.63 (m, 2H), 7.39 (t, J = 7.4 Hz, 2H), 7.32 (t, J = 7.3 Hz, 1H), 6.35 (s, 1H), 4.10 (tt, J = 12.3, 3.9 Hz, 1H), 3.84 (t, J = 9.1 Hz, 1H), 2.21 (qd, J = 12.5, 3.3 Hz, 2H), 1.85 (d, J = 9.7 Hz, 6H), 1.68 (t, J = 11.8 Hz, 4H), 1.61–1.13 (m, 10H). **¹³C NMR** (101 MHz, CDCl₃) δ 152.7, 142.8, 136.1, 132.8, 130.5, 129.0, 128.9, 113.1, 57.0, 52.0, 33.9, 28.6, 26.1, 26.0, 25.3, 24.5. **IR**: 2930, 2855, 1797, 1670, 1647, 1450, 1367, 1331, 1232, 1201, 1089. **HRMS (ESI):** calcd for $C_{22}H_{28}N_2O_2$: 353.2224 $[M + H]^+$. Found: 353.2212 $[M + H]^+$.

Conflicts of interest

There are no conflicts to declare.

Acknowledgements

Notes and references

1 (a) K. S. Lackner, *Science*, 2003, **300**, 1677–1678; (b) P. G. Jessop, D. J. Heldebrant, X. Li, C. A. Eckert and C. L. Liotta, *Nature*, 2005, **436**, 1102; (c) S. H. Kim, K. H. Kim and S. H. Hong, *Angew. Chem., Int. Ed.*, 2014, **53**, 771–774; (d) D. M. Reiner, *Nat. Energy*, 2016, **1**, 15011.

2 (a) Q. Yan and Y. Zhao, *J. Am. Chem. Soc.*, 2013, **135**, 16300–16303; (b) F. Inagaki, C. Matsumoto, T. Iwata and C. Mukai, *J. Am. Chem. Soc.*, 2017, **139**, 4639–4642.

3 C. Villiers, J. P. Dognon, R. Pollet, P. Thuery and M. Ephritikhine, *Angew. Chem., Int. Ed.*, 2010, **49**, 3465–3468.

4 (a) M. A. Dureen and D. W. Stephan, *J. Am. Chem. Soc.*, 2010, **132**, 13559–13568; (b) L. J. Hounjet, C. B. Caputo and D. W. Stephan, *Angew. Chem., Int. Ed.*, 2012, **51**, 4714–4717; (c) C. Das Neves Gomes, E. Blondiaux, P. Thuery and T. Cantat, *Chem. – Eur. J.*, 2014, **20**, 7098–7106; (d) A. Adenot, N. von Wolff, G. Lefevre, J. C. Berthet, P. Thuery and T. Cantat, *Chem. – Eur. J.*, 2019, **25**, 8118–8126.

5 L. F. B. Wilm, T. Eder, C. Muck-Lichtenfeld, P. Mehlmann, M. Wunsche, F. Buss and F. Dielmann, *Green Chem.*, 2019, **21**, 640–648.

6 (a) L. J. Murphy, K. N. Robertson, R. A. Kemp, H. M. Tuononen and J. A. C. Clyburne, *Chem. Commun.*, 2015, **51**, 3942–3956; (b) H. Zhou and X. Lu, *Sci. China: Chem.*, 2017, **60**, 904–911.

7 (a) H. A. Duong, T. N. Tekavec, A. M. Arif and J. Louie, *Chem. Commun.*, 2004, 112–113; (b) H. Zhou, W.-Z. Zhang, C.-H. Liu, J.-P. Qu and X.-B. Lu, *J. Org. Chem.*, 2008, **73**, 8039–8044; (c) Y. Kayaki, M. Yamamoto and T. Ikariya, *Angew. Chem., Int. Ed.*, 2009, **48**, 4194–4197; (d) Y. B. Wang, Y. M. Wang, W. Z. Zhang and X. B. Lu, *J. Am. Chem. Soc.*, 2013, **135**, 11996–12003; (e) H. Zhou, R. Zhang and X.-B. Lu, *Adv. Synth. Catal.*, 2019, **361**, 326–334.

8 (a) F. Buss, P. Mehlmann, C. Muck-Lichtenfeld, K. Bergander and F. Dielmann, *J. Am. Chem. Soc.*, 2016, **138**, 1840–1843; (b) P. Rotering, L. F. B. Wilm, J. A. Werra and F. Dielmann, *Chem. – Eur. J.*, 2020, **26**, 406–411.

9 (a) Y. Tsutsumi, K. Yamakawa, M. Yoshida, T. Ema and T. Sakai, *Org. Lett.*, 2010, **12**, 5728–5731; (b) Y.-B. Wang, D.-S. Sun, H. Zhou, W.-Z. Zhang and X.-B. Lu, *Green Chem.*, 2014, **16**, 2266–2272.

10 (a) K. Vazdar, R. Kunetskiy, J. Saame, K. Kaupmees, I. Leito and U. Jahn, *Angew. Chem., Int. Ed.*, 2014, **53**, 1435–1438; (b) E. D. Nacsa and T. H. Lambert, *J. Am. Chem. Soc.*, 2015, **137**, 10246–10253.

11 (a) C. Das Neves Gomes, O. Jacquet, C. Villiers, P. Thuery, M. Ephritikhine and T. Cantat, *Angew. Chem., Int. Ed.*, 2012, **51**, 187–190; (b) S. Zhang and L.-N. He, *Aust. J. Chem.*, 2014, **67**, 980–988; (c) Z. Xin, C. Lescot, S. D. Friis, K. Daasbjerg and T. Skrydstrup, *Angew. Chem., Int. Ed.*, 2015, **54**, 6862–6866; (d) N.-K. Kim, H. Sogawa, K. Yamamoto, Y. Hayashi, S. Kawauchi and T. Takata, *Chem. Lett.*, 2018, **47**, 1063–1066; (e) G. Li, J. Chen, D. Y. Zhu, Y. Chen and J. B. Xia, *Adv. Synth. Catal.*, 2018, **360**, 2364–2369; (f) C. Zhang, Y. Lu, R. Zhao, W. Menberu, J. Guo and Z. X. Wang, *Chem. Commun.*, 2018, **54**, 10870–10873.

12 (a) M. Yamashita, K. Goto and T. Kawashima, *J. Am. Chem. Soc.*, 2005, **127**, 7294–7295; (b) S. Choi, J. H. Drese, P. M. Eisenberger and C. W. Jones, *Environ. Sci. Technol.*,

2011, **45**, 2420–2427; (c) A. Goeppert, M. Czaun, G. K. Surya Prakash and G. A. Olah, *Energy Environ. Sci.*, 2012, **5**, 7833–7853; (d) T. M. McDonald, W. R. Lee, J. A. Mason, B. M. Wiers, C. S. Hong and J. R. Long, *J. Am. Chem. Soc.*, 2012, **134**, 7056–7065; (e) A. Kumar, D. G. Madden, M. Lusi, K. J. Chen, E. A. Daniels, T. Curtin, J. J. t. Perry and M. J. Zaworotko, *Angew. Chem., Int. Ed.*, 2015, **54**, 14372–14377; (f) E. S. Sanz-Perez, C. R. Murdock, S. A. Didas and C. W. Jones, *Chem. Rev.*, 2016, **116**, 11840–11876; (g) F. M. Brethomé, N. J. Williams, C. A. Seipp, M. K. Kidder and R. Custelcean, *Nat. Energy*, 2018, **3**, 553–559; (h) C. J. E. Bajamundi, J. Koponen, V. Ruuskanen, J. Elfving, A. Kosonen, J. Kauppinen and J. Ahola, *J. CO$_2$ Util.*, 2019, **30**, 232–239; (i) X. Shi, H. Xiao, H. Azarabadi, J. Song, X. Wu, X. Chen and K. S. Lackner, *Angew. Chem.*, 2019, **59**, 6984–7006; (j) S. P. Singh, P. Hao, X. Liu, C. Wei, W. Q. Xu, N. Wei, X. Li, H. Lu and A. Y. Ku, *Joule*, 2019, **3**, 2154–2164.

13 (a) D. J. Heldebrant, P. G. Jessop, C. A. Thomas, C. A. Eckert and C. L. Liotta, *J. Org. Chem.*, 2005, **70**, 5335–5338; (b) B. R. Van Ausdall, J. L. Glass, K. M. Wiggins, A. M. Aarif and J. Louie, *J. Org. Chem.*, 2009, **74**, 7935–7942; (c) C. A. Seipp, N. J. Williams, M. K. Kidder and R. Custelcean, *Angew. Chem., Int. Ed.*, 2017, **56**, 1042–1045.

14 (a) M. Luo, X. H. Zhang and D. J. Darensbourg, *Acc. Chem. Res.*, 2016, **49**, 2209–2219; (b) J. Ying, H. Wang, X. Qi, J.-B. Peng and X.-F. Wu, *Eur. J. Org. Chem.*, 2018, 688–692; (c) J. Ying, C. Zhou and X.-F. Wu, *Org. Biomol. Chem.*, 2018, **16**, 1065–1067.

15 M. Vlasse, S. Giandinoto, S. T. Attarwala, Y. Okamoto and T. J. Emge, *Acta Crystallogr., Sect. C: Cryst. Struct. Commun.*, 1986, **42**, 487–490.

16 M. T. C. Ang, L. Phan, A. K. Alshamrani, J. R. Harjani, R. Y. Wang, G. Schatte, N. J. Mosey and P. G. Jessop, *Eur. J. Org. Chem.*, 2015, 7334–7343.

17 N. von Wolff, C. Villiers, P. Thuéry, G. Lefèvre, M. Ephritikhine and T. Cantat, *Eur. J. Org. Chem.*, 2017, 676–686.

18 (a) T. Sakakura, J.-C. Choi and H. Yasuda, *Chem. Rev.*, 2007, **107**, 2365–2387; (b) Z.-Z. Yang, L.-N. He, Y.-N. Zhao, B. Li and B. Yu, *Energy Environ. Sci.*, 2011, **4**, 3971–3975; (c) Z.-Z. Yang, L.-N. He, J. Gao, A.-H. Liu and B. Yu, *Energy Environ. Sci.*, 2012, **5**, 6602–6639; (d) M. Aresta, A. Dibenedetto and A. Angelini, *Chem. Rev.*, 2014, **114**, 1709–1742; (e) C. Martín, G. Fiorani and A. W. Kleij, *ACS Catal.*, 2015, **5**, 1353–1370; (f) J. Wang and Y. Zhang, *ACS Catal.*, 2016, **6**, 4871–4876; (g) B. Grignard, S. Gennen, C. Jerome, A. W. Kleij and C. Detrembleur, *Chem. Soc. Rev.*, 2019, **48**, 4466–4514; (h) Z. Zhang, X.-Y. Zhou, J.-G. Wu, L. Song and D.-G. Yu, *Green Chem.*, 2019, **22**, 28–32; (i) S. Kar, A. Goeppert and G. K. S. Prakash, *Acc. Chem. Res.*, 2019, **52**, 2892–2903.

19 X. F. Liu, X. Y. Li, C. Qiao, H. C. Fu and L. N. He, *Angew. Chem., Int. Ed.*, 2017, **56**, 7425–7429.

20 (a) J. W. Clark-Lewis, *Chem. Rev.*, 1958, **58**, 63–99; (b) R. L. Dow, B. M. Bechle, T. T. Chou, D. A. Clark, B. Hulin and R. W. Stevenson, *J. Med. Chem.*, 1991, **34**,

1538–1544; (*c*) Y. Momose, T. Maekawa, T. Yamano, M. Kawada, H. Odaka, H. Ikeda and T. Sohda, *J. Med. Chem.*, 2002, **45**, 1518–1534; (*d*) K. Evason, C. Huang, I. Yamben, D. F. Covey and K. Kornfeld, *Science*, 2005, **307**, 258–262; (*e*) J. M. Cox, H. D. Chu, C. Yang, H. C. Shen, Z. Wu, J. Balsells, A. Crespo, P. Brown, B. Zamlynny, J. Wiltsie, J. Clemas, J. Gibson, L. Contino, J. Lisnock, G. Zhou, M. Garcia-Calvo, T. Bateman, L. Xu, X. Tong, M. Crook and P. Sinclair, *Bioorg. Med. Chem. Lett.*, 2014, **24**, 1681–1684.